Highly Stable RNA Capture by Dense Cationic Polymer Brushes for the Design of Cytocompatible, Serum-Stable SiRNA Delivery Vectors

Danyang Li[†,§], *Amir S. Sharili*[†,‖], *John Connelly*[†,‖], *Julien E. Gautrot*[*,†,§]

[†]Institute of Bioengineering and [§]School of Engineering and Materials Science, Queen Mary University of London, Mile End Road, London E1 4NS, United Kingdom

[‖]Barts and the London School of Medicine and Dentistry, Queen Mary University of London, 4 Newark Street, London E1 2AT, United Kingdom

KEYWORDS: Polymer brush, block copolymer, grafting density, gene delivery, siRNA

ABSTRACT

The high density of polymer brushes confers to these coatings unique physico-chemical properties, in particular for the regulation of biomolecular interaction and the design of highly selective coatings for biosensors and protein patterning. Here we show that high density poly(dimethylaminoethyl methacrylate) cationic polymer brushes enable the stable uptake of high levels of oligonucleotides. This is proposed to result from the high degree of crowding and associated increase in entropic driving force for the binding of polyelectrolytes such as nucleic acid molecules. We further demonstrate the ease with which such coatings allow the design of highly structured nanomaterials for siRNA delivery using block copolymer-brush based

nanoparticles that allow the protection of oligonucleotides by a protein resistant outer block. In particular these nanomaterials display a high serum stability and low cytotoxicity whilst retaining excellent knock down efficiencies. Polymer brush-based nanomaterials therefore appear particularly attractive for the rational design of a new generation of high performance theranostics and RNA delivery probes.

INTRODUCTION

Polymer brushes have attracted considerable attention, due to their ease of synthesis via controlled radical polymerizations, offering unprecedented control over the coating structure and architecture[1-2]. Brushes have been applied in the biomedical field for the design of highly specific biosensors and the restriction of protein adsorption and cell adhesion[3]. The very dense crowding of polymer brushes has proved extremely important to reduce protein adsorption to surfaces, beyond detection levels. This has enabled their use for the design of bacterial resistant coatings[4-6] and the patterning of protein and cell adhesions at the nano- to micro-scale[7-10]. In contrast, despite the exceptional level of control of structure and architecture that can be achieved using polymer brushes, including their potential for the design of theranostic probes and the systematic study of nanoparticle-cell interactions, polymer brush-functionalised nanomaterials have found limited applications in drug and gene delivery, perhaps as a result of their limited loading capacity. However, plasmid DNA and RNA (siRNA and miRNA) delivery typically only require very low loading levels (a few copies per cell) [11-12]. Hence a few articles have recently reported the delivery of plasmid DNA using polymer brush-functionalised nanoparticles. For example poly(dimethylaminoethyl methacrylate) (PDMAEMA) brushes were grown from ATRP initiator functionalized silsesquioxane[13], silica nanoparticles[14], nanodiamond[15], gold nanomaterials[16] and

magnetic nanoparticle[17] cores for the capture and delivery of plasmid DNA. Although moderate gene transfection efficiencies were obtained (up to 55% in some cases), one of the key advantages of polymer brushes is to enable the introduction of cores with different chemistry, shapes and sizes (e.g. for imaging properties via fluorescence[14-15] or MRI[16, 18-19]), whilst retaining the same coating chemistry. Therefore polymer brush decorated nanomaterials offer exciting opportunities for the systematic study of parameters impacting gene delivery and transfection (core type, brush chemistry, thickness and grafting density). However, relatively poor infiltration of large plasmid DNA molecules (4.5 kbp) through PDMAEMA brushes[14] implies sub-optimal loading and limits the design freedom of brush-based delivery vectors.

Here we report the high loading level of small RNA molecules within densely packed PDMAEMA brushes and their stabilization via multiple interactions within such highly crowded polycationic environment. Indeed, in contrast to low density polymer coatings typically achieved via a "grafting to" approach, the grafting density of polymer brushes grown via surface initiated polymerization techniques is not limited by thermodynamically controlled surface adsorption, but is determined by the initiator density deposited and the kinetic control of polymerization and termination reactions. As a result of such structural control, we report the use of PDMAEMA brush-functionalized nanoparticles with high knock down efficiency. In addition, we demonstrate the high flexibility of structural design of such nanomaterials, using block copolymer brushes, for their stabilization in complex protein mixtures such as sera and the reduction of cytotoxicity.

EXPERIMENTAL SECTION

Materials. 2-(Dimethylamino)ethyl methacrylate (DMAEMA, Mn = 157.21), oligo(ethylene glycol methyl ether methacrylate) (OEGMA, M_n = 300), copper chloride (Cu(I)Cl), copper bromide (Cu(II)Br_2), 2,2'-bipyridyl (bipy), anhydrous toluene, triethylamine (Et_3N) and 1-undecanethiol were purchased from Sigma-Aldrich and used as received. All chemicals and solvents were analytical grades unless otherwise stated. Cu(I)Cl was kept under vacuum until used. Silicon wafers (100 mm diameter, <100> orientation, polished on one side/reverse etched) were purchased from Compart Technology Ltd and cleaned in a Plasma System Zepto from Diener Electronic, for 10 min in air. Gold-coated substrates were obtained through the evaporation of a chromium layer (20 nm followed by the evaporation of a gold layer (200 nm) using an Edwards Auto 500 evaporator. Silica particles (unfunctionalised) were purchased from Bangs Laboratories (supplied as powder, mean diameters of 300 nm). The thiol initiator, ω-mercaptoundecyl bromoisobutyrate was synthesised according to the literature[20], and silane initiator, (3-trimethoxysilyl)propyl 2-bromo-2-methylpropionate was purchased from Gelest. Surface plasmon resonance (SPR) chips (10 x 12 x 0.3 mm) were purchased from Ssens. Triton X-100, gelatin, phallodin–tetramethylrhodamine B isothiocyanate, PFA (paraformaldehyde), DAPI (4,6-diamidino-2-phenylindole), phosphate buffered saline (PBS, 150 mM) were purchased from Sigma Aldrich. Dulbecco's Modified Eagle Medium (DMEM) medium, OPti-MEM™ medium, Fetal Bovine Serum (FBS), trypsin, versene, penicillin-streptomycin, L-glutamine, Alexa Fluor goat anti-rabbit 488 and DNA fragmens were from Thermo-Fisher. Collagen type I was from BD Bio-science. GFP siRNA (target sequence CGG CAA GCT GAC CCT GAA GTT CAT), EGFR siRNA (target sequence CAG GAA CTG GAT ATT CTG AAA), negative control (NC) siRNA (N/A) were purchased from Qiagen®. The EGFP plasmid was purified by using a plasmid

purification kit from PureLink™, thermo fisher. Anti-EGFR monoclonal antibody (rabbit) was purchased from Abcam. Western blot gel, buffers, transfer kit and protein ladder were purchased from Bio-Rad. Secondary IRDye® 800CW Donkey anti-Rabbit IgG (H + L) was from Li-cor.

Polymer brush synthesis on flat surfaces (silicon wafer, gold substrate and SPR chips)

The brushes were synthesised from the bromo initiator moieties with the 'grafting from' method, using atom transfer radical polymerisation (ATRP).

Deposition of the ATRP silane initiator on silicon wafers. A piece of plasma-oxidized silicon wafer was immersed in a solution of silane initiator (30 μL), Et_3N (50 μL), anhydrous toluene (30 mL), and left at room temperature overnight. Then the wafer was rinsed with ethanol and dried under nitrogen stream. Initiator-coated wafers were kept in a dry and dust free nitrogen box until needed. The dry thickness of silane initiator layers was near 2 nm, as measured via spectroscopic ellipsometry (JA Woollam, -SE).

Deposition of ATRP thiol initiator on gold substrates and SPR chips. Gold substrate and SPR chips were first plasma-oxidised and immersed in 5 mM thiol initiator ethanoic solutions containing two different ratios of ω-mercaptoundecyl bromoisobutyrate to 1-undecanethiol (100 % and 10 %, depending on the grafting density targeted). The chips were left at room temperature overnight, then washed with ethanol and dried under nitrogen. The thiol initiator functionalised chips were used to grow polymer brushes freshly. The dry thickness of thiol initiator layers was near 2 nm, as measured via ellipsometry.

Synthesis of PDMAEMA brushes. To study PDMAEMA brush growth and the evolution of its thickness as a function of time, a solution of $CuBr_2$ (18 mg, 80 μmol), bipy (320 mg, 2.05 mmol), and DMAEMA (42 mmol, 6.6 g) in water/ethanol (4/1 (v/v), 30 mL) was degassed using argon bubbling for 30 min. CuCl (82 mg, 828 μmol) was added into this solution quickly and the resulting mixture was sonicated to ensure fully dissolve of CuCl and further degassed for 30 min before polymerization. Initiator-coated silicon/gold substrates (~1 × 1 cm^2 each) were placed in reaction vessels and degassed via four cycles of high vacuum/nitrogen gas refilling. Subsequently, 1 mL of DMAEMA solution was transferred to reaction vessels under inert atmosphere via a syringe. The polymerization was stopped at different time points (2.5, 5, 10, 20, 30 min) by immersing the coated substrates in deionized water, followed by washing with copious amounts of ethanol and drying under a nitrogen stream. The dry thickness of PDMAEMA brush was measured via ellipsometry afterwards. PDMAEMA brush growth kinetics can be found in Fig. S1. For the preparation of sparse PDMAEMA brushes on gold substrates, the thiol initiator was diluted with 1-undecanethiol at a ratio of 1:9. Brush thickness on undiluted and diluted thiol monolayers can be found in Fig. S2.

Synthesis of POEGMA brushes. The procedure of POEGMA brush synthesis was similar as for PDMAEMA brushes except for the difference in monomer solution: the OEGMA solution consisted $CuBr_2$ (18 mg, 80 μmol), bipy (320 mg, 2.05 mmol), and OEGMA (42 mmol, 12.6 g) and CuCl (82 mg, 828 μmol) in water/ethanol (4/1 (v/v), 30 mL). Kinetics for POEGMA brush growth was also studied at time points of 2.5, 5, 10, 20, 30 min. POEGMA brush growth kinetics can be found in Fig. S10.

Synthesis of block copolymer brush (BCB). For preparation of block copolymer brush, 1 mL DMAEMA solution (composition is the same as in 1.2.1) was add to each reaction vessel

containing the initiator-coated silicon wafers, gold substrates or SPR chips under inert atmosphere. After polymerisation for the time corresponding to the targeted thickness (10 nm, 4 min polymerization, or 30 nm, 20 min polymerization), according to PDMAEMA brush growth kinetics in Figure S1), 10 mL of OEGMA monomer solution (composition is the same as in 1.2.2) was injected and left to polymerise for different time points before the reaction was stopped. Total dry thicknesses were measured afterwards by ellipsometry. Growth kinetics for the second block can be found in Fig. S11.

Synthesis of polymer brush coated silica nanoparticles

Initiator deposition. Anhydrous toluene (4 mL) kept under nitrogen was added to 200 mg 300 nm silica nanoparticles. The particles were sonicated for 10 min and were shaken until the suspension turned cloudy and homogenous. The silica particles were then centrifuged at 4000 rpm x 15 min and the toluene was aspirated out. The sonication and centrifugation process was repeated three times and the particles were finally dispersed in 4 mL anhydrous toluene. The initiator grafting process was carried out by adding 200 µL Et_3N, 40 µL silane initiator to the 4 mL silica dispersion and stirring overnight. Then the silica particles with silane initiator (SiO_2-silane) were washed with 4 mL ethanol three times and stored in final water/ethanol (4/1 (v/v), 10 mL)) in the fridge until needed for polymerization.

Synthesis of PDMAEMA brushes on silica nanoparticles (SiO_2-PDMAEMA). The polymerization solution was prepared as described previously by dissolving DMAEMA (6.6 g, 42 mmol), bipy (320 mg, 2.05 mmol), $CuBr_2$ (80 mmol) and CuCl (0.082 g, 828 µmol) in half of the total polymerization solvent (water/ethanol 4/1 (v/v), 15 mL). 10 mL SiO_2-silane dispersion obtained

in 2.1 were degassed for 30 minutes with argon bubbling while stirring. An equal volume of DMAEMA monomer solution was added to the SiO_2-silane suspension. Polymerization was allowed to proceed under argon at RT for 20 min to get 30 nm of PDMAEMA brush on SiO_2. To terminate the polymerization, the particle dispersion was diluted using deionized water and bubbled with air until the color changed from dark brown to blue (oxidization of CuCl). The particles were recovered via centrifugation, washed successively with water and ethanol to get rid of the catalysts and residual monomer, during which, sonication was applied to reduce the aggregation and finally the particles were dispersed in 10 mL deionized water and stored in the fridge.

Synthesis of POEGMA brushes on silica nanoparticles (SiO_2-POEGMA). The procedure of POEGMA brush synthesis was similar to that used for PDMAEMA brushes except for the difference in monomer solution. For OEGMA polymerization on silica nanoparticles, the monomer solution was: OEGMA (12.6 g, 42 mmol), bipy (320 mg, 2.05mmol), $CuBr_2$ (80 mmol) and CuCl (0.082 g, 828 µmol) in 15 mL solvent (water/ethanol 4/1 (v/v), 15 mL).

Synthesis of block copolymer brushes on silica nanoparticles (SiO_2-BCB). For preparation of block copolymer brushes on silica nanoparticles, 2.5 mL DMAEMA monomer solution described in 2.2.1 was added to an equal volume of degassed SiO_2-silane dispersion under inert atmosphere. After achieving 30 nm of PDMAEMA brush (polymerisation for 20 min), 50 mL OEGMA monomer solution described in 2.2.2 was injected and left to polymerise for 120 min according to Figure S11 to generate a second block containing POEGMA and PDMAEMA (molar ratio of 10) with a thickness of 30 nm. Polymerisation was stopped and particles were purified in the same way as for SiO_2-PDMAEMA, as described in 2.2.1.

Polymer brush coated nanoparticle characterization

Size and zeta potential measurement. The size and zeta potential of PDMAEMA, POEGMA and block copolymer brush coated silica nanoparticles were measured with a Malvern zetasizer nano ZS. Samples were prepared by dispersing particles in PBS until obtaining a slightly cloudy solution and then sonicated for 10 min with shaking at regular intervals. Each samples were measured in triplicates (three independent samples from at least two batches of particles) at 25°C and the average result was taken as the final hydrodynamic diameter or zeta potential.

Thermogravimetric (TGA) measurement. By using TGA, the dry mass of polymer on silica nanoparticles was determined. Herein, the TGA was performed in air using a TA Instruments Q500. All samples were heated from room temperature to up to 1000 °C at a heating rate of 10 °C/min and dried under vacuum at room temperature prior to TGA runs. It was assumed that the mass change from 100 °C to 900 °C was due to the burning of the organic polymer brush coatings and the remainder was non-combustible silica particles. The polymer brush thickness on silica nanoparticles was calculated according to TGA results in Fig. S6 and equation S3.

Fourier transform infrared - attenuated total reflectance (FTIR-ATR). FTIR was used to characterise the different chemical groups expected within the respective materials through obtaining an infrared spectrum. ATR-FTIR spectroscopy in this study was carried out using a Bruker Tensor 27 with an MCT detector (liquid N2 cooled). Spectra were taken at a resolution of 4 cm^{-1} with a total of 128 scans per run. FTIR spectroscopy was carried out on bare SiO_2, SiO_2-PDMAEMA, SiO_2-POEGMA and SiO_2-BCB, results in Fig. 4C.

Brush density measurement on silica nanoparticles. PDMAEMA brush density on silica nanoparticles can be determined by Equation S4, knowing the weight percentage (characterised by TGA) and molecular weight of PDMAEMA on silica nanoparticles. For molecular weight characterization, PDMAEMA was cleaved from silica nanoparticles and characterized with gel permeation chromatography (GPC). Briefly, 5 mL SiO_2-PDMAEMA particle suspension (20 mg/mL) was added to 25 mL 10 % hydrofluoric acid solution and stirred at room temperature for 4 h. The cloudy particle suspension turned clear after silica cores dissolved completely. The solution was then transferred to a 3.5 KD Spectra/Por® dialysis bag, dialyzed with deionized water and freeze dried afterwards. GPC measurements were carried on an Agilent 1260 infinity system operating in dimethylformamide (DMF) with 5 mM ammonium tetrafluoroborate at 50 °C and equipped with refractive index detectors and variable wavelength detectors. The instrument was calibrated with linear narrow polystyrene standards in a range of 550 to 46,890 g/mol. 2 mg of PDMAEMA cleaved from silica nanoparticles was dissolved in 2 mL of DMF completely and filtered before GPC characterization.

Transmission electron microscopy (TEM). TEM measurements were carried out using a JEOL 2010 transmission electron microscope with a LaB6 filament, operated at 200 kV. Samples were prepared by dropping the diluted brush coated silica nanoparticle suspension on a copper grid with porous carbon film and drying at room temperature.

Characterisation of interactions between polymer brushes and nucleic acids via SPR

SPR was used to evaluate the interaction between nucleic acid molecules (10 bp DNA, 100 bp DNA, 22 bp RNA and 4.5 kbp plasmid) and polymer brushes with a Biacore 3000. SPR chips were

coated with polymer brushes prior to mounting on a substrate holder. Mounted chips were docked, primed with PBS and equilibrated with PBS at 10 μL/min flow rate until a stable baseline was obtained. 50 μL nucleic acid solutions (plasmid DNA or RNA) were injected at 10 μg/mL. Once the injection was finished, washing with PBS was continued at 10 μL/min flow rate. The nucleic acid adsorption level was measured after washing with PBS for 15 min. Nucleic acid adsorption studies via SPR was carried out with chips coated with 30 nm brushes, at densities of 100 % and 10 % for PDMAEMA, POEGMA brushes and 100 % density of block copolymer brush (PDMAEMA, 10 nm, + POEGMA, 10 nm). All measurements were carried out in triplicates (three separate chips freshly prepared).

Characterisation of protein adsorption to polymer brushes and nanoparticle aggregation

Proteins adsorption to polymer brush coated SPR chips. SPR was used to investigate the binding of proteins on polymer brushes. Similar methods to those used for the characterisation of nucleic acid adsorption were used, but chips were exposed to 50 μL of 10 % FBS during injection of the protein samples. Measurements were carried on 10 nm PDMAEMA, POEGMA brushes and 100 % density of block copolymer brushes (PDMAEMA, 10 nm, + POEGMA, 10 nm). All measurements were carried out in triplicates (three separate chips freshly prepared).

Nanoparticle and siRNA complex aggregation in serum solutions. SiO_2-PDMAEMA, SiO_2-POEGMA, SiO_2-BCB and their siRNA complexes (N/P of 10) were dispersed in 10 % FBS (PBS) solution for 30 min, 2 h, 24 h and 48 h respectively. Subsequently, particles were centrifuged and washed three times and redispersed in PBS before characterisation via DLS. Changes in size after

incubation in FBS solutions indicated the aggregation of particles following protein adsorption. Each sample was measured in triplicate at 25°C.

Cell viability assay

HaCaT Cell culture and passage. DMEM media supplied with 10 % FBS, 1 % Penicillin-Streptomycin (P/S) and 1 % glutamine was used to culture HaCaT cells in 37^{o}C/5 % CO_2 incubator. To harvest HaCaT cells (T75), cells were washed twice with pre-warmed PBS solution and then cells were detached from the flask by trypsinisation (versene/trypsin, 4/1 v/v, 5 mL, 37°C). 15 mL of DMEM medium was then added to the flask to quench the trypsin. Cells were transferred to a 50 mL centrifuge tube and centrifuged at 1200 rpm for 5 min. After discarding the supernatant solution, the pellet was resuspended in 10 mL FAD medium and the concentration of cells was measured with a haematocytometer.

Cell viability test. Cells were seeded at a density of 50 k cells per well (in 500 µL of DMEA medium) in 24-well plates 24 h prior. SiRNA (with a final concentration of 50 nM/well) complexed with SiO_2-PDMAEMA, SiO_2-POEGMA, SiO_2-BCB at N/P=5, 10, 15 and Lipofectamine/siRNA were added into each well for 4 h in serum free OPTI-MEM medium and then the medium was replaced by full culture DMEM medium for further 24 h incubation. Cell viability was carried out by live/dead assay in which, cells were incubated in 500 µL DMEM medium of 4 mM calcein AM and 2 mM ethidium homodimer for 30 min prior to imaging. Fluorescence imaging was used to capture the live-dead cells and these were counted via ImageJ to obtain the percentage of live cells of total number of cells.

Transfection assay

Establishment of stable HaCaT Cells expressing green fluorescence protein (HaCaT-GFP). Stable HaCaT cell lines expressed EGFP-actin were generated by transfection with linearized plasmids for EGFP-actin (Clontech, Mountain View, CA) as previously described[21]. Cells were transfected using Lipofectamine 2000 according to the manufacturer's instructions and selected with 0.5 mg/mL G418 until a stable GFP positive population was established.

Knock down assay with SiO_2-PDMAEMA and SiO_2-BCB. The protocol for culturing and passaging HaCaT-GFP cells was the same as for HaCaT cells. HaCaT-GFP cells were seeded at a density of 50 k/well on glass cover slips pre-treated with collagen in 24 well plates, 24 h prior to the transfection assay. A final siRNA concentration of 50 nM/well was used for all transfection assays described in this report. 100 µL SiO_2-PDMAEMA/GFP siRNA (or SiO_2-BCB/GFP siRNA) complexes were prepared at N/P=5, 10 and 15, in serum free OPTI-MEM medium. After removing the DMEM medium, cells were washed twice with pre-warmed serum free OPTI-MEM medium and another 400 µL was added. 100 µL siRNA complex was then added dropwise to each well and mixed by shaking gently. Cells were incubated with siRNA complexes for 4 h in the incubator and the medium was then replaced by 500 µL full culture DMEM medium for a further 24 h of incubation. Lipofectamine® 2000 complexed with GFP siRNA/negative control (NC) siRNA (protocol according to the manufacturer's instruction with a final siRNA concentration of 50 nM/well) was used as a positive/negative control. The transfected cells were washed with PBS three times, fixed in paraformaldehyde (PFA, 4 %, 10 min) and permeabilised with Triton X-100 (0.2 %, 5 min). Cells were then stained with TRITC-phalloidin (1:1000) and DAPI (4,6-diamidino-2-phenylindole, 1:1000) in blocking buffer (10% FBS and 0.25% gelatin from cold water fish skin,

Sigma-Aldrich) and kept at room temperature for 1 h. Cover slips with fixed cells were mounted on glass slides before imaging with a Leica DMI4000 fluorescence microscope.

SiO_2-BCB/EGFR siRNA on cancer cells (immunostaining and western blot). Cancer cells used in this study were HeLa cells and A549 cells. The culture medium and protocol were similar with HaCaT cells except for shorter trypsinisation times. Both cancer cells were transfected with SiO_2-BCB/EGFR siRNA, lipofectetamine/EGFR siRNA and lipofectetamine/NC siRNA at N/P ratio of 10. After transfection, cells were washed with PBS, fixed and permeabilised as described in 7.1. Non-specific protein binding was blocked by incubating the cover-slips for 1 h in blocking buffer (10% FBS and 0.25% gelatin in PBS). Subsequently, the cover-slips were incubated with anti-EGFR monoclonal antibody (anti-EGFR, 1:200, Abcam) in blocking buffer for 1 h at room temperature. After washing with PBS three times, cells were then incubated with Alexa Fluor 488-conjugated secondary antibody (goat anti-rabbit, 1:1000, Thermo-Fisher), phalloidin (1:1000) and DAPI (1:1000) in blocking buffer for 1 h at room temperature. Samples were washed and mounted onto glass slides prior to imaging. The relative protein abundance across samples was determined for western blot. After transfection, cells were harvested, lysised and the protein content was quantified (Pierce™ BCA Protein Assay Kit, Thermo-Fisher). Equal protein loadings was further confirmed by GAPDH. Bands were separated on a 4% to 15% SDS-PAGE gradient gels (Bio-Rad) and semi-dry transferred on to PVDF membranes. Blots were incubated with blocking buffer (5 % milk powder and 5 % FBS in TBS buffer) at room temperature for 1 h before incubating with an anti-EGFR monoclonal antibody 1:1000 (identical to that used for immunostaining) in blocking buffer at 4 °C overnight. After washing three times with TBS + tween buffer, secondary IRDye® 800CW Donkey anti-Rabbit IgG (H + L) (1:15000, Li-cor) in blocking buffer was applied for a

further 1 h incubation at room temperature. Bands were visualized using an Odyssey® imaging system (Li-cor).

Statistics

Data are reported as averages ± stdev for groups of at least three replicates, or as individual values with the average indicated. An unpaired, two-tailed Student's t test was used for assessing of statistical significance (*$p<0.05$, **$p<0.01$, ***$p<0.001$).

RESULT AND DISCUSSION

Controlled polymer brush growth on flat surfaces

The growth kinetics of PDMAEMA brushes generated via ATRP was investigated first, both on silicon wafers and gold substrates to confirm the control of brush growth from silica-type materials and SPR chips (gold coated on glass). Progress of the polymerisation was monitored by characterising the dry brush thickness via ellipsometry (Figure S1). The brush growth rate can be controlled by varying the monomer concentration, the ratio of Cu(I) to Cu(II), the nature of the ligands, and the solvent composition. In this study, addition of ethanol resulted in particularly well-controlled growth of PDMAEMA brush especially for thin brushes below 45 nm, as the PDMAEMA brush thickness profile is linear with little initial jump. Moreover, by diluting the initiator with its non-reactive analogues, the desired grafting density of PDMAEMA can be easily achieved according to Equation 1:

$$\sigma = \frac{\rho_m N_A h_{dry}}{M_n} \quad \text{(Equation 1)}$$

where ρ_m is the density of DMAEMA (1.318 g/cm^3), N_A is Avogadro's number, h_{dry} is the dry thickness of the brushes, and M_n is the average molecular weight of the tethered polymer chains [22-23].

Monitoring the interaction of PDMAEMA brush with nucleic acids

The interactions of double stranded DNA and RNA probes with PDMAEMA brushes was investigated via surface plasmon resonance (SPR), in order to establish how brush density and nucleic acid probe size control their interactions and infiltration. To investigate the role of grafting density on such interactions, the density of PDMAEMA brushes was controlled by diluting the silane ATRP initiator with an unreactive silane (Figure S2). The adsorption of DNA probes, with sizes ranging from 10 to 4.5 kbp and a 22 bp RNA probe, to PDMAEMA brushes was monitored via SPR (Figure 1A and B). On dense brushes (0.50 chains/nm^2 [22-24]), fast adsorption was observed for all probes, but in particular for the shorter 10 bp DNA and 22 bp RNA molecules. Upon washing with phosphate-buffered saline (PBS), stable retention was observed, except for the smallest DNA probe, implying a weaker entropic drive for the adsorption of such small molecules. In contrast, the adsorption profile of nucleic acid molecules to lower density brushes (0.12 chains/nm^2) displayed no significant differences in the initial rate of adsorption (with the exception of the large plasmid DNA), followed by a relatively fast desorption upon washing with PBS, in particular for the 10 bp DNA probe. Hence our results imply that nucleic acid adsorption to polymer brushes is kinetically limited by molecular crowding but results in considerable stabilization of adsorbed nucleic acid molecules with intermediate sizes. In all cases, the calculated negative charge density (phosphates) of molecules adsorbed remained significantly lower (< 7,800

pmol/cm^2 for 22 bp RNA Figure 1C) than the positive charge density measured for high density PDMAEMA brushes (26,500 pmol/cm^2). Therefore, in polymer brushes, molecular crowding, and local desorption/re-adsorption phenomena[25], combine to entropic stabilization (including a strong component resulting from counterion release), resulting in stable retention of the corresponding molecules (Figure 1D). Entropic stabilization of oligonucleotides may also be enhanced in polymer brushes, due to the frustrated conformation of polymer chains. Surprisingly, this effect was particularly pronounced in the case of 22 bp RNA molecules (Figure 1C), perhaps as a result of additional hydroxyl groups and the presence of uridyl bases present on RNA probes[26]. The short length and stiffer structure of RNA molecules, compared with larger DNA molecules and plasmids, is typically though to reduce interactions and condensation, with cationic polymeric non-viral delivery agents.[27-29] Consequently, a higher N/P ratio is typically required to form polyplexes with siRNA molecules, to optimize knock down efficiencies.[27] Therefore the dense crowding of cationic polymer brushes constitutes a unique environment for highly stable RNA uptake.

Synthesis and characterization of PDMAEMA brush coated silica nanoparticles

The high binding capacity of RNA probes within dense PDMAEMA brushes suggested their use for siRNA delivery and the regulation of gene expression. Firstly, PDMAEMA brush coated 300 nm silica nanoparticles (SiO_2-PDMAEMA, measured with DLS in PBS) were prepared via ATRP with well dispersed particle size of 443 ± 6 nm in PBS (Figure S3) and zeta potential of 15.8 ± 4.4 mV. Our previous work showed that PDMAEMA brush growth from silica particles is well controlled at the targeted thickness[14]. The morphology of SiO_2-PDMAEMA was confirmed by transmission electron microscope (TEM, Figure S4), which displayed an obvious organic layer of

PDMAEMA surrounding the silica core. The associated changes in surface chemistry were confirmed by fourier transform infrared spectroscopy (FTIR, Figure S5), with the appearance of a band at 1730 cm^{-1}, characteristic of C=O vibrations for PDMAEMA. The amount of PDMAEMA on the surface of SiO_2 was determined by thermogravimetric analysis (TGA) analysis, with 24 % weight loss associated with the polymer coating (Table1 and Figure S6). According to Equation 2, the dry brush thickness of PDMAEMA brushes on SiO_2 was calculated as 28 nm. After cleavage of PDMAEMA chains from silica nanoparticles by hydrofluoric acid, the resulting PDMAEMA was characterized by gel permeation chromatography (GPC in Figure S7) and using Equation 3. The PDMAEMA chain density on SiO_2 was found to be 0.45 chain/nm^2, close to the dense brushes achieved on flat silicon wafers. Thus, dense PDMAEMA brush coated silica nanoparticles were prepared for further siRNA knock down studies.

$$h = R\left(\frac{W_{brush}\rho_{SiO_2}}{W_{SiO_2}\rho_{brush}} + 1\right)^{1/3} - R \quad \text{(Equation 2)}$$

Equation 2 was used to determine the brush thickness on silica nanoparticles, where W_{brush} is the weight loss percentage corresponding to the decomposition of polymer brush component, W_{SiO2} is the residual weight percentage, ρ_{brush} is the mass density of polymer brush ($\rho_{PDMAEMA,}$ 1.318 g/cm^3, $\rho_{POEGMA,}$ 1.105 g/cm^3), ρ_{SiO2} is the density of bulk SiO_2 (2.4 g/cm^3), R is the radius of SiO_2 (150 nm).

$$\delta = \frac{\frac{W_{PDMAEMA}}{W_{SiO_2}}\rho_{SiO_2}V_{SiO_2}N_A}{M_{PDMAEMA}S_{SiO_2}} \quad \text{(Equation 3)}$$

Equation 3 was used to determine the PDMAEMA brush density on silica nanoparticles, where $W_{PDMAEMA}$ is the weight loss percentage corresponding to the decomposition of PDMAEMA, W_{SiO2} is the residual weight percentage, ρ_{SiO2} is the density of bulk SiO_2 (2.4 g/cm^3), V_{SiO2} is the volume of SiO_2 nanoparticle calculated from the average diameter of SiO_2 (300 nm), N_A is Avogadro's number, $M_{PDMAEMA}$ is the molecular weight of PDMAEMA cleaved from SiO_2, and

S_{SiO2} is the surface area of SiO_2 nanoparticle calculated from the average diameter of SiO_2 (300 nm)[30].

SiO_2-PDMAEMA knocking down efficiency and cell viability

A keratinocytes cell line expressing actin-GFP was selected for simple quantification of siRNA efficiency, using GFP siRNA (allowing simultaneous imaging of endogenous and GFP-tagged actin after phalloidin staining for quantification). Knock down levels were determined for different N/P ratios (5, 10 and 15) and compared to the commercialized transfection agent lipofectamine 2000 as a positive control. The fluorescent intensity ratio of GFP (green)/ phalloidin (red) was measured and compared with the ratio of non-transfected cells to determine the knock down efficiency. Highest knock down efficiencies (66 ± 6 %) were measured at N/P=10, comparable with those measured with lipofectamine (Figure 2A and 2B), whilst there was no significant increase in transfection levels at N/P=15. In comparison, green fluorescence in the blank and negative control (NC) siRNA groups remained unaltered (Figure S8). However, the toxicity of SiO_2-PDMAEMA/siRNA complexes was found to be lower than that of lipofectamine (Figures 2C), in which cell viability at N/P=5 or 10 were maintained above 65 % (full set of images can be found in Figure S9). Indeed the inherent toxicity of cationic vectors remains an important issue to address in the field of gene delivery[31-32] via non-viral cationic vectors. In addition, cationic vectors typically display poor stability in complex protein solutions, such as serum and blood, limiting the bloodstream circulation time and translation of these technologies[33].

Design of block copolymer brush-based nanoparticles

In order to address simultaneously cytotoxicity and stability issues, we developed a double shell approach enabling the coating of the PDMAEMA shell with a protein resistant and cytocompatible POEGMA shell[9, 34-36], to reduce protein adsorption and shield cell membranes from toxic cationic moieties. However, despite the wide range of block copolymer brushes generated and studied on flat substrates[1, 37], few reports have presented the synthesis of block copolymer brushes from nanoparticles[38]. In addition, "grafting to" approaches do not allow high grafting densities suitable for stable RNA loading (Figure 1). Hence we re-initiated POEGMA blocks from the PDMAEMA first shell on both flat surfaces and silica nanoparticles (Figure 3) via the growth of a mixed PDMAEMA/POEGMA block (1/10 ratio, particles designated as SiO_2-BCB). Ellipsometry was used to characterize dry brush thickness of block copolymer brushes generated from silicon substrates (Figure S10 and S11), indicating the good control of brush re-initiation from both 10 and 30 nm PDMAEMA brushes. SiO_2-BCB (silica nanoparticles with grafted block copolymer brushes) displayed a hydrodynamic radius of 550 ± 14 nm, as determined by DLS (Figure 4A), and a zeta potential of 4.4 ± 2.4 mV, considerably reduced compared with SiO_2-PDMAEMA. Additionally, FTIR (Figure 4C) spectra of SiO_2-PDMAEMA and SiO_2-BCB displayed characteristic bands of PDMAEMA (C-H stretching of amines) at 2767 cm^{-1} and 2820 cm^{-1} whereas SiO_2-POEGMA and SiO_2-BCB displayed bands characteristics of (C-H stretching characteristic of POEGMA) at 2870 cm^{-1}, further indicating the successful sysnthesis of SiO_2-BCB particles. In addition, an increased organic polymer layer (double the thickness) was observed by TEM (Figure 4B), in agreement with TGA analysis (Figure S6), confirming the increased dry brush thickness (Table 1) of SiO_2-BCB.

We then characterized RNA loading within the block copolymer brushes generated (Figure5). SPR experiments demonstrated that 22 bp RNA molecules rapidly diffused through the outer block of the brush and bound to the PDMAEMA block at levels comparable to those measured for mono-block PDMAEMA brushes. We confirmed that POEGMA brushes did not bind any detectable level of RNA. RNA binding was further evidenced by light scattering experiments, which indicated increases in brush thickness and reduction in zeta potential for SiO_2-POEGMA and SiO_2-BCB but not SiO_2POEGMA (Supplementary Table S1). Similarly the protein absorption of the block copolymer brushes synthesized reduced by about 50 %, compared to pure PDMAEMA brushes, in good agreement with differential adsorption to PDMAEMA and POEGMA brushes from serum[7-8, 35]. Therefore our results indicate that a block copolymer brushes reduce significantly protein adsorption whilst retaining high levels of RNA uptake.

Serum stability and cell viability of SiO_2-BCB nanoparticles

The potential of SiO_2-BCB particles to improve the safe delivery of siRNA to cells and to resist to aggregation and destabilization in complex protein solutions was evaluated. We first characterized the stability of these colloids in 10% FBS solutions (Figure 6A), from 30 min to 48 h via DLS. SiO_2-POEGMA particles were also prepared and characterized using the same protocol, as negative control (anti-fouling POEGMA brushes resist protein adsorption and confer colloidal stability). In agreement with the high level of protein adsorption measured by SPR from 10% FBS solutions (Figure 5C), SiO_2-PDMAEMA particles aggregated and sedimented rapidly (with charge reversal +16 mV to -5 mV) within 30 mins. In comparison, SiO_2-POEGMA and SiO_2-BCB particles did not display notable signs of aggregation (Figure 6A), even after 48 h (Figure S12). In

addition, we monitored changes in particle sizes for complexes formed at N/P of 10 (see Supplementary Figure S13), which were used in transfection assays. As for pristine particles, serum stability was investigated by incubation of siRNA complexes in 10 % FBS solutions. No obvious aggregation was observed for SiO_2-BCB/siRNA and SiO_2-POEGMA/siRNA complexes. In contrast, for SiO_2-PDMAEMA/siRNA, although after binding with siRNA part of the positive charge from PDMAEMA brushes was shielded, a marked increase in particle size was observed after short periods of incubation, followed by aggregation at later time points. The cytotoxicity of SiO_2-BCB remained low (96 ± 4 % viability at an N/P of 10), in contrast to that observed for SiO_2-PDMAEMA and lipofectamine in Figure 2C. Full set of images were displayed in Figure S9). Together, these results demonstrate that the addition of a POEGMA outer block to the PDMAEMA brush significantly improves cell viability, in addition to particle stability in the presence of serum.

SiO_2-BCB-mediated knock down actin-GFP and EGFR

To determine whether SiO_2-BCB retained a high siRNA delivery efficiency, their knock down performance was assessed in our HaCaT-GFP model. Similar transfection levels (near 60 %) were measured with SiO_2-BCB (N/P=10), SiO_2-PDMAEMA (N/P=10) and lipofectamine (Figure 7). In contrast, no reduction level was observed in any of our controls (Figure 7B and S13). Therefore, the addition of a POEGMA outer block did not prevent siRNA delivery and knock down of the targeted gene, despite the expected reduction in cell membrane interactions, perhaps as a result of the residual positive zeta potential of SiO_2-BCB particles.

To demonstrate the application of our brush-based vectors, we investigated their use for the knock down of edpidermal growth factor receptors (EGFR) in cancer cells, receptors often overexpressed

in epithelial malignancies[39-40]. Gene therapy and knock down of EGFR would allow the reduction of tumor growth, in combination to other therapeutic strategies[41]. An optimized N/P ratio of 10 was used as in the case of SiO_2-BCB/EGFR siRNA. Glyceraldehyde 3-phosphate dehydrogenase (GAPDH) was used as internal loading control. No obvious EGFR knock down was observed in groups of blank cells and Lipofectamine/NC siRNA (non-targeting) complex. In contrast, transfection of EGFR siRNA with SiO_2-BCB nanoparticles allowed efficient knock down of EGFR in HeLa and A549 non-small lung carcinoma cells (western blotting results in Figure 8A and 8B). Immunofluorescence microscopy further confirmed the reduction in the expression of EGFR (Figure 8C). EGFR in non-transfected cells or cells transfected with the negative control siRNA was clearly visible at the cell membrane and within the cytoplasm, whereas cells transfected with SiO_2-BCB/EGFR siRNA displayed reduced levels of EGFR, in agreement with western blots. Hence block copolymer brush-based vectors are versatile agents for efficient knock down of genes for the treatment of diseases and molecular biology studies

CONCLUSIONS

In conclusion, we showed that the binding of nucleic acid molecules to cationic polymer brushes depends both on brush density and size of the nucleic acid sequence. We demonstrated that such brushes can be applied to the design of nanoparticles displaying a combination of high knock down efficiency, improved protein resistance and solution stability, as well as low cytotoxicity. In addition to the ease with which polymer brushes can be functionanlised with bioactive moieties (to confer targeting for example) from a wide range of nanomaterials conferring imaging capability, degradability or responsive behavior, such block copolymer brush siRNA delivery

vectors are attractive candidates for the design of a new generation of therapeutic platforms. Improving our understanding of parameters (chemical and structural) regulating such RNA-brush interactions, and the stable assembly and dissociation of RNA molecules from brush-based vectors, should enable the improved design of new RNA delivery platforms.

ASSOCIATED CONTENT

Supporting Information.

Additional ellipsometry, TEM, DLS, FTIR, TGA, GPC data and additional images of knock down experiments and cell viability assays.

AUTHOR INFORMATION

Corresponding Author

j.gautrot@qmul.ac.uk

Author Contributions

DL carried out experiments. ASS prepared the plasmid and reviewed the manuscript. DL, JC and JEG prepared the manuscript.

Notes

The authors declare no competing financial interests.

ACKNOWLEDGMENT

We thank Dr. Nadezda Tarakina and Mr. Russel Bailey for assisting TEM imges in this article. Funding from the China Scholarship Council (No.201406240022) for Danyang Li's studentship is gratefully acknowledged.

REFERENCES

(1) Barbey, R.; Lavanant, L.; Paripovic, D.; Schuwer, N.; Sugnaux, C.; Tugulu, S.; Klok, H. A. *Chem. Rev.* **2009,** *109,* 5437-5527.
(2) Edmondson, S.; Osborne, V. L.; Huck, W. T. *Chem. Soc. Rev.* **2004,** *33,* 14-22.
(3) Krishnamoorthy, M.; Hakobyan, S.; Ramstedt, M.; Gautrot, J. E. *Chem. Rev.* **2014,** *114,* 10976-11026.
(4) Cheng, G.; Zhang, Z.; Chen, S.; Bryers, J. D.; Jiang, S. *Biomaterials* **2007,** *28,* 4192-4199.
(5) Li, G.; Xue, H.; Cheng, G.; Chen, S.; Zhang, F.; Jiang, S. *J. Phys. Chem. B* **2008,** *112,* 15269-15274.
(6) Rzhepishevska, O.; Hakobyan, S.; Ruhal, R.; Gautrot, J.; Barbero, D.; Ramstedt, M. *Biomater. Sci.* **2013,** *1,* 589-602.
(7) Gautrot, J. E.; Trappmann, B.; Oceguera-Yanez, F.; Connelly, J.; He, X.; Watt, F. M.; Huck, W. T. S. *Biomaterials* **2010,** *31,* 5030-5041.
(8) Ma, H.; Hyun, J.; Stiller, P.; Chilkoti, A. *Adv. Mater.* **2004,** *16,* 338-341.
(9) Gautrot, J. E.; Wang, C.; Liu, X.; Goldie, S. J.; Trappmann, B.; Huck, W. T. S.; Watt, F. M. *Biomaterials* **2012,** *33,* 5221-5229.
(10) Di Cio, S.; Bøggild, T. M. L.; Connelly, J.; Sutherland, D. S.; Gautrot, J. E. *Acta Biomater.* **2017,** *50,* 280-292.
(11) Mello, C. C.; Conte, D. *Nature* **2004,** *431,* 338-342.
(12) Carthew, R. W.; Sontheimer, E. J. *Cell* **2009,** *136,* 642-655.
(13) Schallon, A.; Synatschke, C. V.; Jérôme, V.; Müller, A. H. E.; Freitag, R. *Biomacromolecules* **2012,** *13,* 3463-3474.
(14) Krishnamoorthy, M.; Li, D.; Sharili, A. S.; Gulin-Sarfraz, T.; Rosenholm, J. M.; Gautrot, J. E. *Biomacromolecules* **2017,** *18,* 4121-4132.
(15) Zhang, P.; Yang, J. H.; Li, W. C.; Wang, W.; Liu, C. J.; Griffith, M.; Liu, W. G. *J. Mater. Chem.* **2011,** *21,* 7755-7764.
(16) Yan, P.; Zhao, N.; Hu, H.; Lin, X.; Liu, F.; Xu, F.-J. *Acta Biomater.* **2014,** *10,* 3786-3794.
(17) Majewski, A. P.; Stahlschmidt, U.; Jérôme, V.; Freitag, R.; Müller, A. H. E.; Schmalz, H. *Biomacromolecules* **2013,** *14,* 3081-3090.
(18) Ohno, K.; Mori, C.; Akashi, T.; Yoshida, S.; Tago, Y.; Tsujii, Y.; Tabata, Y. *Biomacromolecules* **2013,** *14,* 3453-3462.
(19) Zeng, H. C. *J. Mater. Chem.* **2011,** *21,* 7511-7526.
(20) Jones, D. M.; Brown, A. A.; Huck, W. T. S. *Langmuir* **2002,** *18,* 1265-1269.
(21) Sharili, A. S.; Kenny, F. N.; Vartiainen, M. K.; Connelly, J. T. *Sci. Rep.* **2016,** *6,* 33893.
(22) Christau, S.; Moller, T.; Yenice, Z.; Genzer, J.; von Klitzing, R. *Langmuir* **2014,** *30,* 13033-13041.
(23) Sanjuan, S.; Perrin, P.; Pantoustier, N.; Tran, Y. *Langmuir* **2007,** *23,* 5769-5778.

(24) Bhat, R. R.; Genzer, J. *Appl. Surf. Sci.* **2006,** *252***,** 2549-2554.
(25) Gautrot, J. E.; Huck, W. T. S.; Welch, M.; Ramstedt, M. *ACS Appl. Mater. Interfaces* **2010,** *2***,** 193-202.
(26) Shen, Z. L.; Xia, Y. Q.; Yang, Q. S.; Tian, W. D.; Chen, K.; Ma, Y. Q. *Top. Curr. Chem.* **2017,** *375*.
(27) Katas, H.; Alpar, H. O. *J. Controlled Release* **2006,** *115***,** 216-225.
(28) Gary, D. J.; Puri, N.; Won, Y. Y. *J. Controlled Release* **2007,** *121***,** 64-73.
(29) Cun, D.; Jensen, L. B.; Nielsen, H. M.; Moghimi, M.; Foged, C. *J. Biomed. Nanotech.* **2008,** *4***,** 258-275.
(30) Chen, J.; Liu, M.; Chen, C.; Gong, H.; Gao, C. *ACS Appl. Mater. Interfaces* **2011,** *3***,** 3215-3223.
(31) Synatschke, C. V.; Schallon, A.; Jerome, V.; Freitag, R.; Muller, A. H. *Biomacromolecules* **2011,** *12***,** 4247-4255.
(32) Huang, Y. Y.; Lin, D. S.; Jiang, Q.; Zhang, W. D.; Guo, S. T.; Xiao, P.; Zheng, S. Q.; Wang, X. X.; Chen, H. B.; Zhang, H. Y.; Deng, L. D.; Xing, J. F.; Du, Q.; Dong, A. J.; Liang, Z. C. *Biomaterials* **2012,** *33***,** 4653-4664.
(33) Hwang, S. J.; Davis, M. E. *Curr. Opin. Mol. Ther.* **2001,** *3***,** 183-191.
(34) Ladd, J.; Zhang, Z.; Chen, S.; Hower, J. C.; Jiang, S. *Biomacromolecules* **2008,** *9***,** 1357-1361.
(35) Tan, K. Y.; Lin, H.; Ramstedt, M.; Watt, F. M.; Huck, W. T. S.; Gautrot, J. E. *Integr. Biol.* **2013,** *5***,** 899-910.
(36) Rodriguez Emmenegger, C.; Brynda, E.; Riedel, T.; Sedlakova, Z.; Houska, M.; Alles, A. B. *Langmuir* **2009,** *25***,** 6328-6333.
(37) Kizhakkedathu, J. N.; Kumar, K. R.; Goodman, D.; Brooks, D. E. *Polymer* **2004,** *45***,** 7471-7489.
(38) He, X. H.; Wu, X. M.; Cai, X.; Lin, S. L.; Xie, M. R.; Zhu, X. Y.; Yan, D. Y. *Langmuir* **2012,** *28***,** 11938-11947.
(39) Normanno, N.; De Luca, A.; Bianco, C.; Strizzi, L.; Mancino, M.; Maiello, M. R.; Carotenuto, A.; De Feo, G.; Caponigro, F.; Salomon, D. S. *Gene* **2006,** *366***,** 2-16.
(40) Sasaki, T.; Hiroki, K.; Yamashita, Y. *Biomed. Res. Int.* **2013,** *2013***,** 546318.
(41) Zheng, D.; Giljohann, D. A.; Chen, D. L.; Massich, M. D.; Wang, X.-Q.; Iordanov, H.; Mirkin, C. A.; Paller, A. S. *Proc. Natl. Acad. Sci.* **2012,** *109***,** 11975-11980.

Figures:

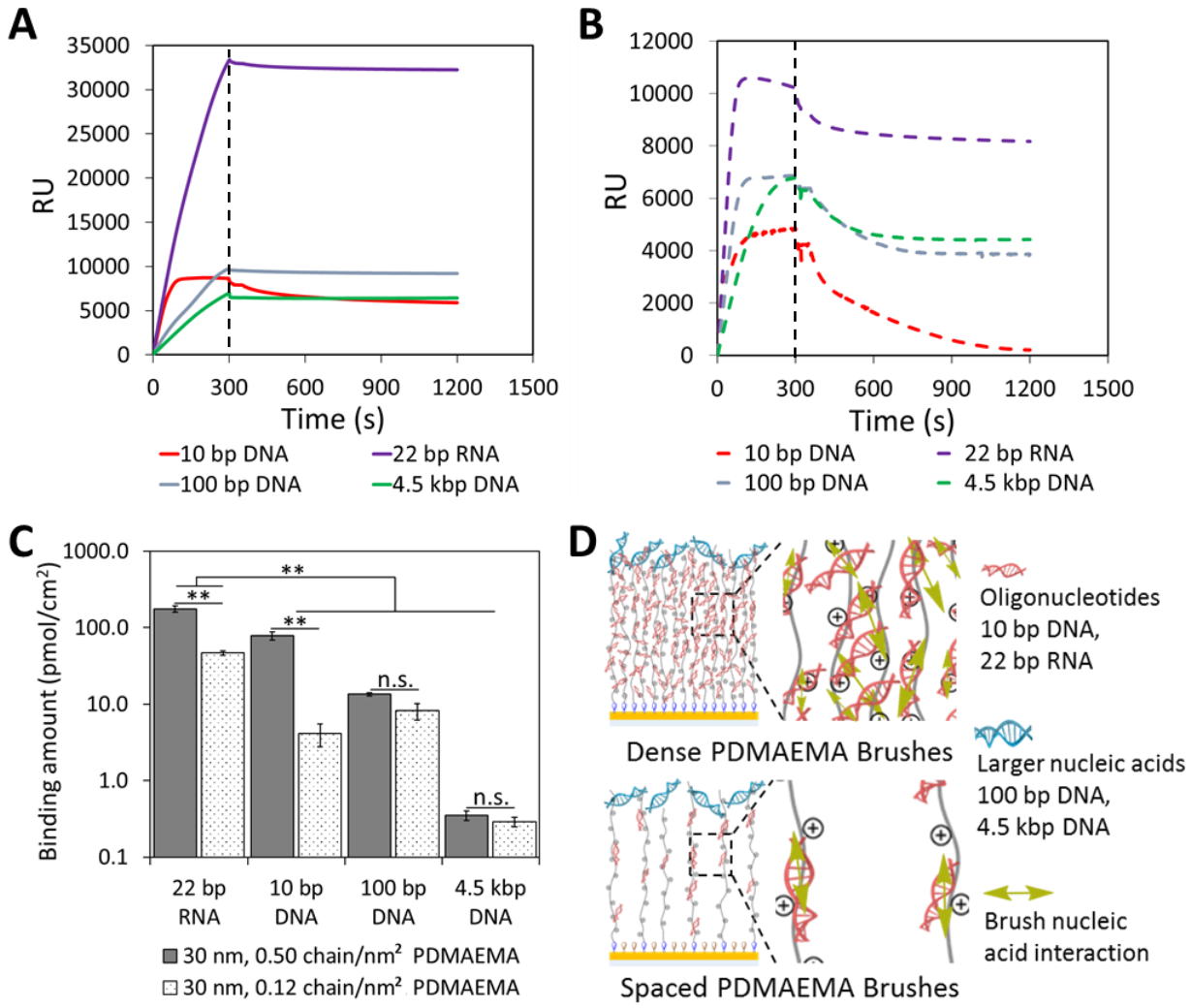

Figure 1. SPR traces for different nucleic acid molecules adsorbing to dense (A) and sparse PDMAEMA brushes (B). After equilibration, nucleic acid solutions were introduced at t = 0 s and stopped after 300 s (dotted lines), followed by washing with PBS. C, Quantification and statistical analysis of nucleic acids binding levels on dense and sparse brushes in A and B. D, Schematic illustration of nucleic acid molecules interacting with PDMAEMA brushes (chain conformations are indicative and only intended to illustrate differences in binding capacity, not thought to be representative of the true brush structure).

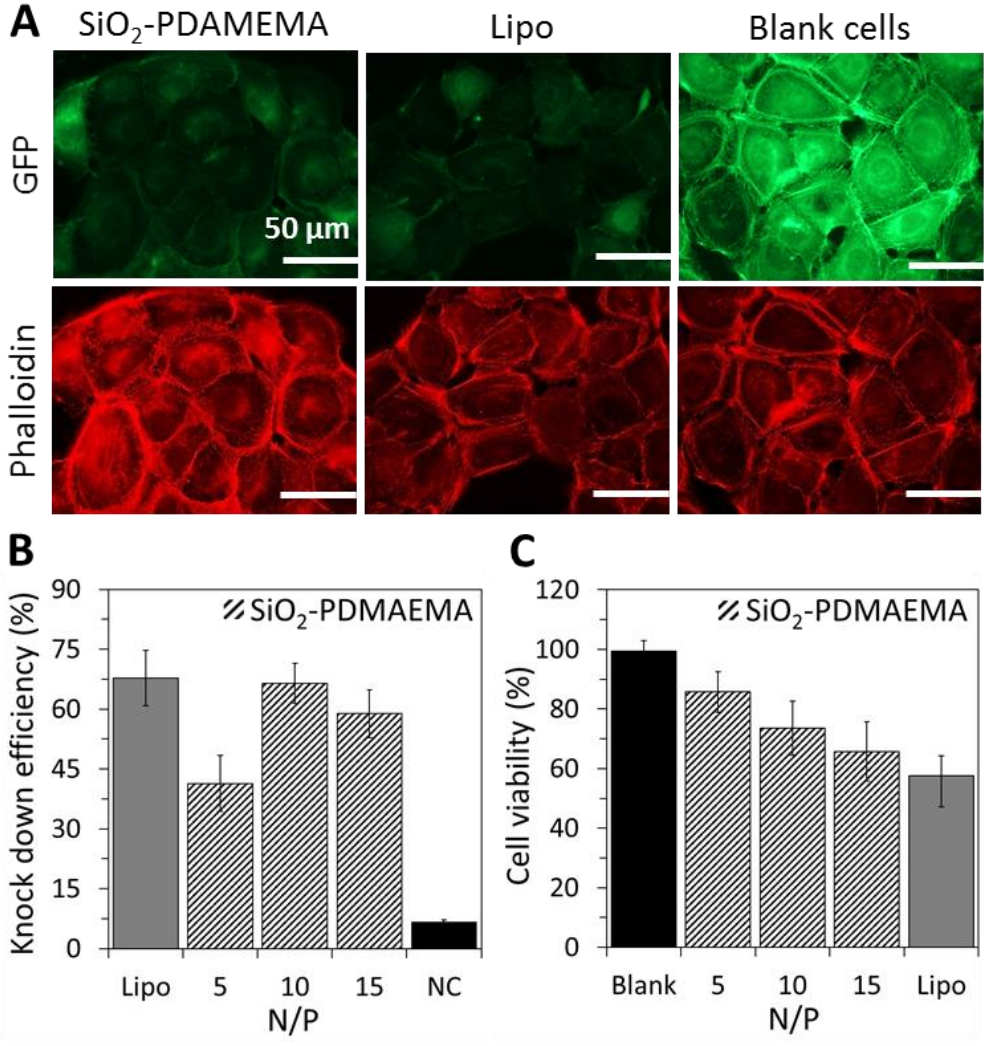

Figure 2. Knock down efficiency of SiO_2-PDMAEMA/GFP siRNA with HaCaT-GFP cells at N/P=5, 10 and 15 compared with Lipofectamine 2000/GFP siRNA (or NC siRNA, 2A and 2B, scale bar: 50 µm); HaCaT cell viability test with live/dead assay on siRNA complexes with different N/P (2C).

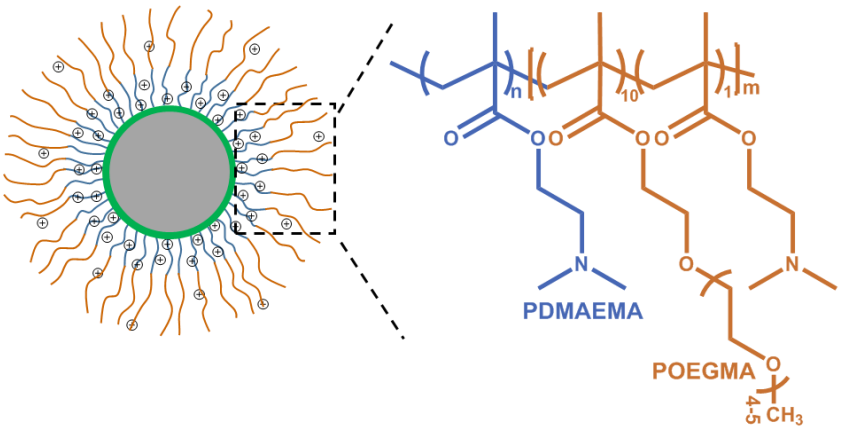

1

2 Figure 3. Schematic illustration and chemical structures of SiO_2-BCB.

3

4

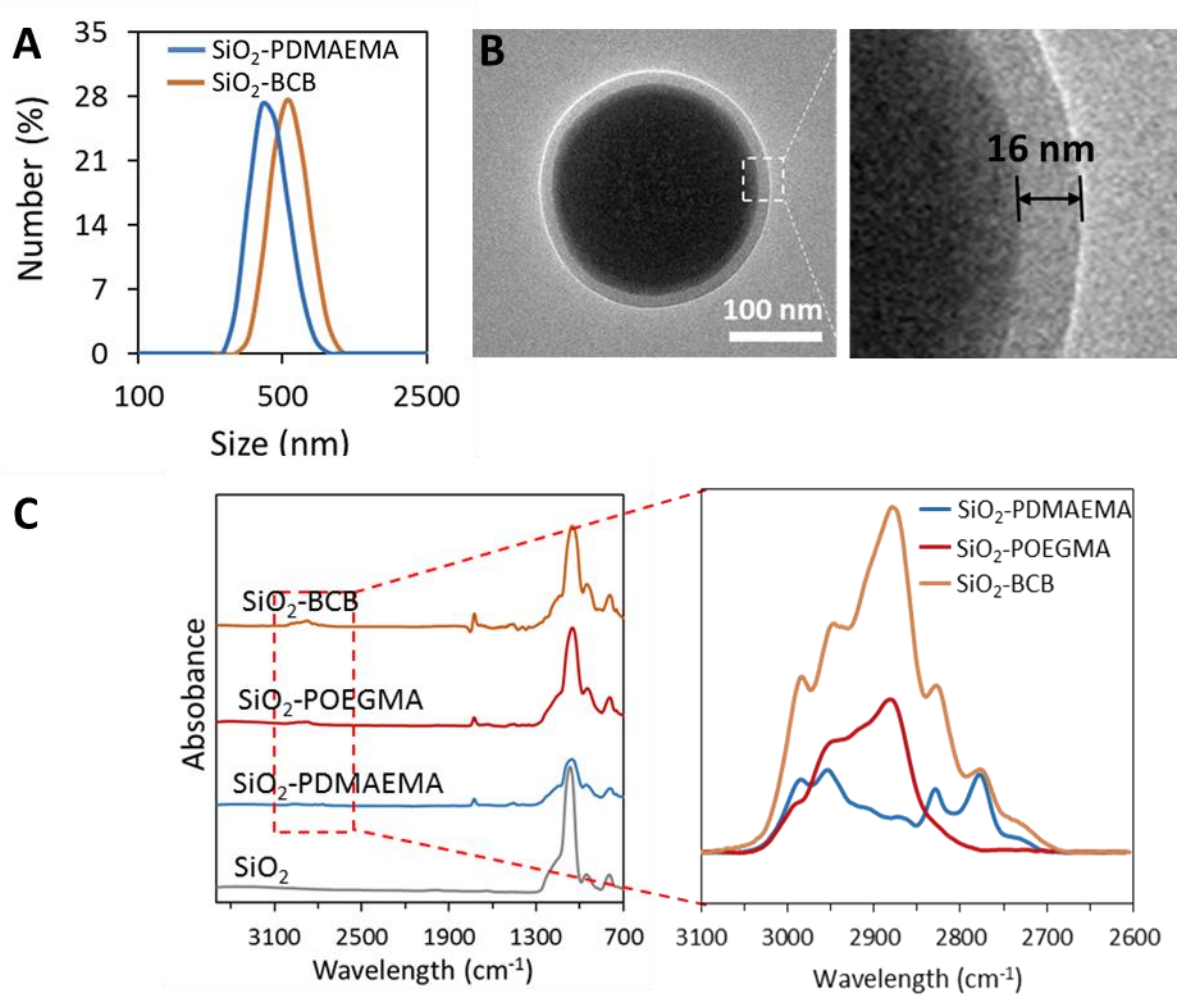

Figure 4. Characterisation size of SiO_2-PDMAEMA and SiO_2-BCB via DLS, in PBS (A); B, TEM image of SiO_2-BCB displaying a 16 nm thick dry block copolymer brush (the inner PDMAEMA block was 8 nm thick, see Figure S4); C, FTIR characterization of SiO_2-BCB.

Table 1.TGA characterization and dry brush thickness on SiO_2.

Sample	Initiator (w %)	PDMAEMA (w %)	POEGMA (w %)	SiO_2 (w %)	PDMAEMA (nm)	POEGMA (nm)
Bare SiO_2	0	0	0	95	0	0
SiO_2-initiator	5	0	0	90	0	0
SiO_2-PDMAEMA	5	24	0	66	28	0
SiO_2-POEGMA	5	0	25	65	0	33
SiO_2-BCB	5	24	14	52	28	25

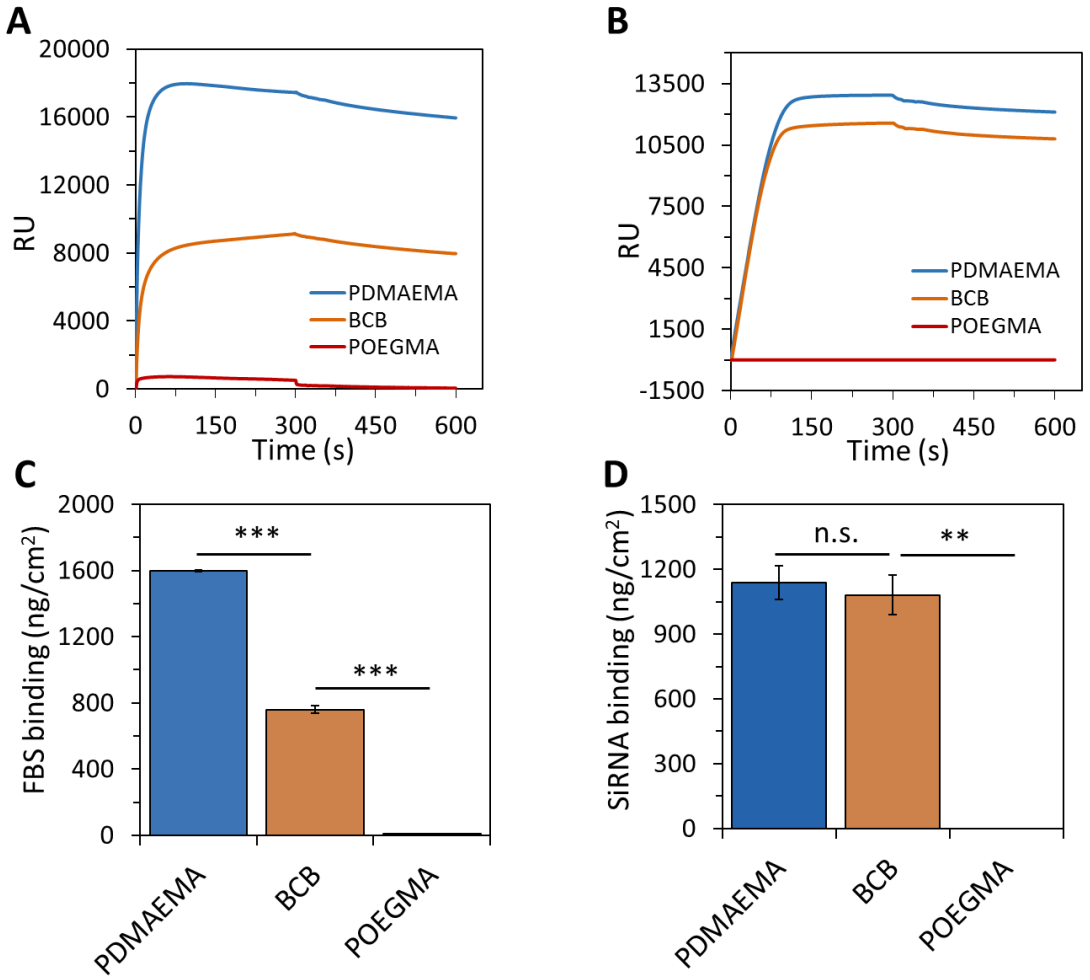

Figure 5. FBS (A and C) and siRNA (B and D) binding levels on PDMAEMA brushes, BCB (10 nm PDMAEMA + 10 nm second block) and POEGMA brushes

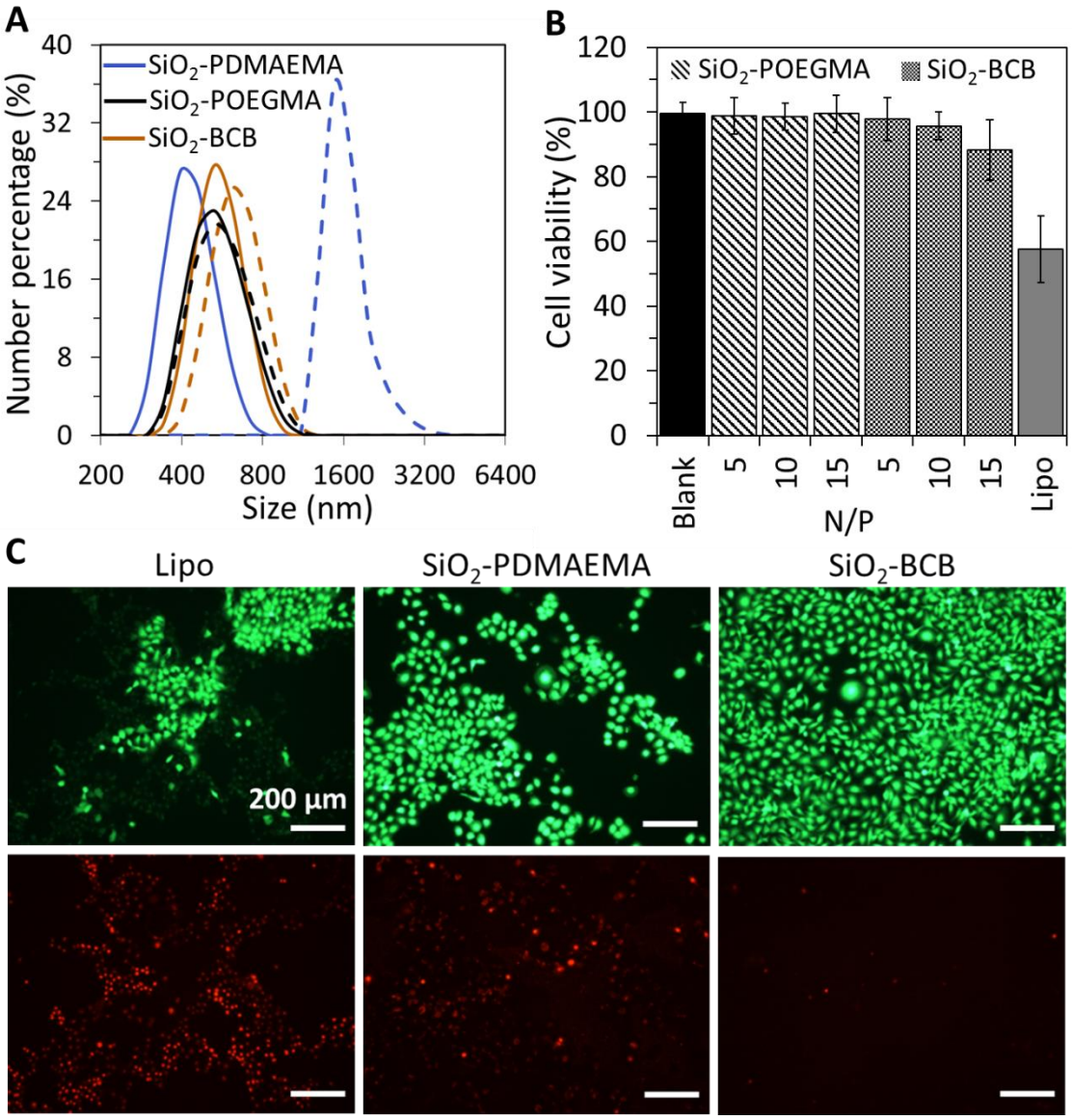

Figure 6. Serum stability of SiO_2-PDMAEMA, SiO_2-BCB and SiO_2-POEGMA (A; DLS, incubation with 10 % FBS, solid line: initial size, dotted line: after incubation in 10 % FBS for 24 h); HaCaT cell viability with SiO_2-POEGMA and SiO_2-BCB/siRNA complexes compared with blank and Lipo/siRNA controls (B and C).

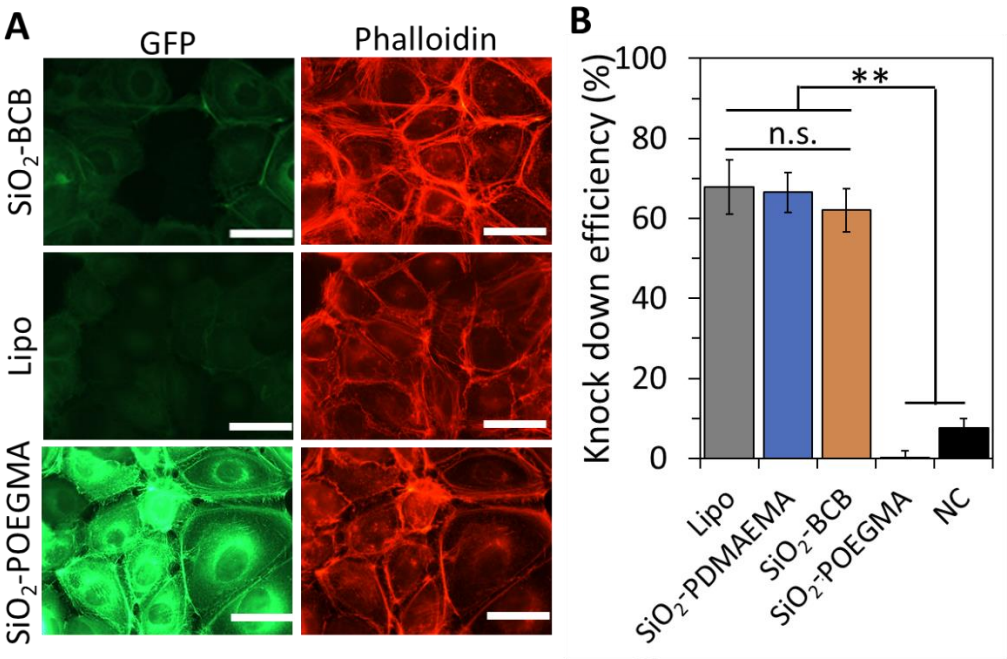

1

2 Figure 7. Knock down efficiency of SiO_2-BCB/GFP siRNA with HaCaT-GFP cells (A and B).

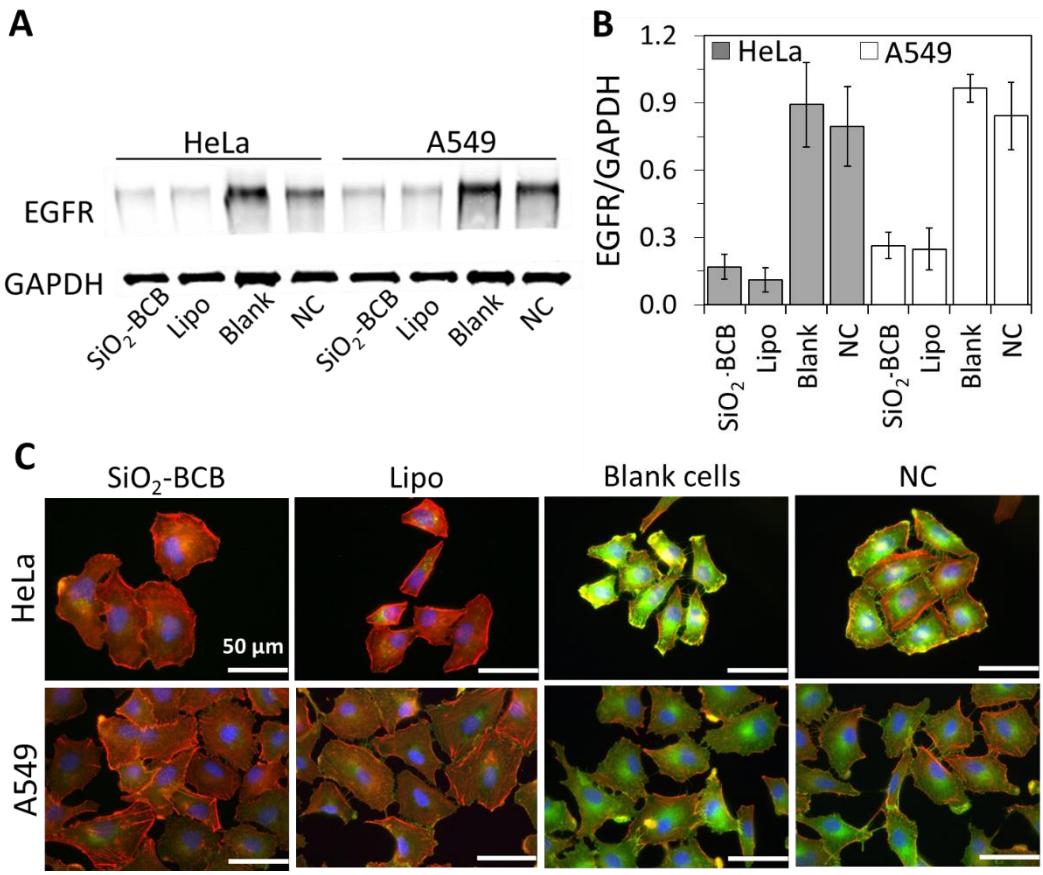

Figure 8. Western blot quantification (A and B) and fluorescent immunostaining (C) of EGFR in HeLa and A549 cells after transfection with SiO_2-BCB/EGFR siRNA.